



# The Effects of Buoyancy, Magnetic Field and Thermal Radiation on the Flow and Heat Transfer due to an Exponentially Stretching Sheet

A'isyah Jaafar<sup>1</sup>, Zanariah Mohd Yusof<sup>2</sup>, Noraini Ahmad<sup>3</sup>, Anuar Jamaludin<sup>1,\*</sup>

<sup>1</sup> Department of Mathematics, Universiti Pertahanan Nasional Malaysia, 57000 Kuala Lumpur, Malaysia

<sup>2</sup> Faculty of Computer and Mathematical Sciences, Universiti Teknologi MARA Kuala Terengganu Campus, 21080 Kuala Terengganu, Malaysia

<sup>3</sup> Centre of Foundation Studies, Universiti Teknologi MARA, Cawangan Selangor, Kampus Dengkil, 43800 Dengkil, Selangor, Malaysia

## ARTICLE INFO

### Article history:

Received 6 September 2022

Received in revised form 8 October 2022

Accepted 11 November 2022

Available online 1 April 2023

### Keywords:

Buoyancy; magnetic field; thermal radiation; exponentially stretching sheet

## ABSTRACT

The boundary layer flow and heat transfer across an exponentially stretched sheet with buoyancy, magnetic field, and thermal radiation are investigated. The similarity transformation is applied to the governing equations to generate nonlinear ordinary differential equations. They are resolved using a numerical technique referred to the Keller-box method. The impact of determined controlling parameters on flow and heat transfer characteristics are investigated. It has been discovered that the buoyancy parameter increases both the heat transfer rate and fluid flow from the exponentially extending sheet to the fluid.

## 1. Introduction

The exponentially stretching sheet that includes the aspects of heat and mass transmission are crucial to industry processes has contributed to many applications such as the metal spinning manufacturing, glass-fiber manufacturing utilizing plastic film, hot rolling production, metal and polymer extraction and wire drawing manufacturing. Throughout engineering and industrial operations, the quality of the final products relies on kinematics expansion and simultaneous heating as well as cooling. The unique properties of the exponentially stretching sheet have piqued the researcher's curiosity, leading to the rapidly increasing number of papers that extending previous knowledge with various aspects of this problem. The exponentially stretching sheet was investigated by Idowu and Usman [1] with viscous fluid, Mushtaq *et al.*, [2] with variable fluid, Loganathan and Vimala [3] with nanofluid, Asghar *et al.*, [4] with hybrid nanofluid, Yusof *et al.*, [5] with Casson fluid, and Abu Bakar and Soid [6] with micropolar fluid.

It is important to know about magnetohydrodynamics (MHD) since it is essential in the process of engineering manufacturers that occur at high temperatures. Rajput *et al.*, [7] said MHD or known as the magnetic field is the study of the interaction Newtonian or non-Newtonian fluid and magnetic properties. The existence of currents in a conductive fluid led to the creation of Lorentz force drag in

\* Corresponding author.

E-mail address: [mohdanuar@upnm.edu.my](mailto:mohdanuar@upnm.edu.my) (Anuar Jamaludin)

<https://doi.org/10.37934/cfdl.15.4.116>

fluid actuate by magnetic field. Mahat *et al.*, [8] stated that the Lorentz force plays a role in determining the flow of fluid. MHD could be found in engineering processes such as nuclear reactors, electromagnetic casting, petroleum refinement and plasma confinement. Furthermore, Ganesan and Palani [9] said that, depending on the significant distinction of the fluid towards the direction perpendicular to the motion and magnetic field, MHD might be used to solve the cooling of nuclear reactors caused by liquid sodium and an induction flow valve. The studies of MHD also gained the interest of Khan *et al.*, [10], Hanafi and Shafie [11], Nayan *et al.*, [12], and Shafique *et al.*, [13].

Thermal radiation can be defined as the emission of energy from a source and travels over some material or space. It is significantly important in the study of controlling heat transfer process, operating temperature, and design of the pertinent equipment in industries. The examples involving engineering areas are nuclear power plants, solar power technology, satellites, missiles, gas turbines, fossil fuel combustion energy process and space vehicles. The study on thermal radiation through an exponentially stretching sheet has been investigated by numerous researchers. The thermal radiation effect was considered by Sajid and Hayat [14] and Bidin and Nazar [15] by applying the numerical solution, Ishak [16] for MHD boundary layer flow, Mukhopadhyay [17] for thermally stratified medium and Mukhopadhyay [18] for MHD boundary layer flow slip effects with suction or blowing.

The study on buoyancy or mixed convection in the fluid flow has given a big impact on science and technology fields thanks to its expanded implementation in many engineering products. The fuel generator of nuclear reactors and the different temperature atmospheric flow are the two examples of mixed convection application. The effects of mixed convection have been studied by Lok *et al.*, [19] under non-orthogonal stagnation point flow, Ishak *et al.*, [20] under stretching vertical surface, Bhattacharyya [21] under the vertical plate, Daniel and Daniel [22] under the viscous fluid flow, Mahat *et al.*, [8] under the viscoelastic nanofluid, Ali *et al.*, [23] under the flow of hybrid nanofluid, and Jahan *et al.*, [24] under a non-isothermal hybrid nanofluid.

The present study expands the work of Ishak [16] by incorporating the influence of buoyancy into the existing permeability equation in the governing equations. This study aims to: (i) use the Keller-box method to establish a numerical scheme for the problem of laminar boundary layer flow and heat transfer across an exponentially stretching sheet in the presence of buoyancy, magnetic, and thermal radiation; and (ii) investigate the impacts of the buoyancy parameter on the surface shear stress of the magnetic parameter, thermal radiation parameter, and Prandtl number. The numerical results for multiple governing parameters are derived and represented graphically. In addition, the numerical comparison results for limited instances are performed using existing released data.

## 2. Mathematical Modelling

Consider a steady two-dimensional boundary layer flow and heat transfer across an exponentially stretching sheet in the influence of buoyancy, magnetic field, and thermal radiation. Under the boundary layer along with the Boussinesq approximations, the governing equations by Ishak [16] was modified into:

$$\frac{\partial u}{\partial x} + \frac{\partial v}{\partial y} = 0, \quad (1)$$

$$u \frac{\partial u}{\partial x} + v \frac{\partial u}{\partial y} = \nu \frac{\partial^2 u}{\partial y^2} - \frac{\sigma B^2}{\rho} u \pm g\beta(T - T_\infty) - \frac{\nu}{D^*} u, \quad (2)$$

$$u \frac{\partial T}{\partial x} + v \frac{\partial T}{\partial y} = \frac{\kappa}{\rho c_p} \frac{\partial^2 T}{\partial y^2} - \frac{1}{\rho c_p} \frac{\partial q_r}{\partial y}, \quad (3)$$

The boundary conditions for this problem are:

$$\begin{aligned} u &= U_w(x), \quad v = 0, \quad T = T_w(x) \quad \text{at} \quad y = 0, \\ u &\rightarrow 0, \quad T \rightarrow T_\infty \quad \text{as} \quad y \rightarrow \infty, \end{aligned} \quad (4)$$

Expression of  $U_w(x)$ ,  $T_w(x)$  and  $B(x)$  are presented in the following form:

$$U_w = U_0 e^{x/L}, \quad T_w = T_\infty + T_0 e^{x/2L}, \quad B(x) = B_0 e^{x/2L}, \quad (5)$$

where  $u$  and  $v$  are the velocity components pointed to the  $x$  and  $y$  directions, and  $T$  is the fluid temperature,  $T_\infty$  is the ambient medium of temperature and mass concentration that was assumed to be linearly stratified.

Following Eq. (2),  $\sigma$  is refer to the fluid electrical conductivity,  $B$  is the magnetic field that adapted normally to the sheet,  $\rho$  is fluid density,  $g$  is the acceleration due to gravity,  $\beta$  is the coefficient of thermal expansion,  $\nu$  is the kinematic viscosity and  $D^*$  is permeability constant. Meanwhile in Eq. (3),  $\kappa$  is refer to the fluid thermal conductivity,  $c_p$  is specific heat at constant pressure, and  $q_r$  is the radiative heat flux. Later in Eq. (4) and Eq. (5),  $U_w$  is the exponential velocity where it manipulates the plate to stretch as  $U_0 > 0$ ,  $T_w$  is the sheet temperature of the stretching surface,  $U_0$  is the reference velocity and  $B_0$  is a constant. The sign of "+" and "-" in Eq. (2) corresponds to the buoyancy parameter's effect on assisting and opposing flow, which illustrates the buoyancy parameter's effect on fluid flow. The physical model and the coordinate system of the flow under a condition where stretching sheet applied can be seen in Figure 1. As fluid flows through a vertically stretched heated sheet, the buoyancy force opposes the lower half of the fluid field and assist the upper half. However, this study will focus on the assisting flow of buoyancy effect toward exponentially stretching sheet. In assisting flow, the  $x$ -axis travels upwards in the direction of the stretched heated surface as the thermal buoyant flow and the stretching induced flow collude. If the surface is cooled under the surrounding temperature, the tendency reverses.

The governing equations of Eq. (1) to Eq. (3) are contingent on boundary conditions in Eq. (4) and being reduced to nonlinear ordinary differential equations under the similarity transformation by Ishak [16] as follows:

$$u = U_0 e^{x/L} f'(\eta), \quad v = - \left( \frac{\nu U_0}{2L} \right)^{\frac{1}{2}} e^{\frac{x}{2L}} [f(\eta) + \eta f'(\eta)], \quad (6)$$

$$T = T_\infty + T_0 e^{x/2L} \theta(\eta), \quad \eta = \left( \frac{U_0}{2\nu L} \right)^{1/2} e^{x/2L} y,$$

where  $\eta$  is the similarity variables and  $\theta$  is the dimensionless temperature.

On using the transformed nonlinear ordinary differential equations are:

$$f''' - 2(f')^2 + ff'' - Mf' + \lambda\theta - Df' = 0, \quad (7)$$

$$\left(1 + \frac{4}{3}R\right)\theta'' + \text{Pr}[f\theta' - f'\theta] = 0, \quad (8)$$

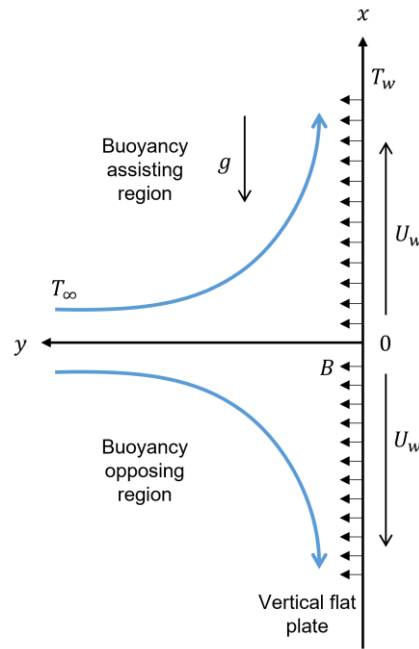


**Fig. 1.** Physical representation and coordinate system under a vertical flat plate

Subject to the boundary conditions:

$$f(0) = 0, \quad f'(0) = 1, \quad \theta(0) = 1 \quad \text{at } \eta = 0, \quad (9)$$

$$f'(\eta) \rightarrow 0, \quad \theta(\eta) \rightarrow 0 \quad \text{as } \eta \rightarrow \infty,$$

where  $M$  represent magnetic field,  $\lambda$  represent buoyancy parameter,  $D$  is the permeability parameter, the Prandtl number is referred to  $\text{Pr}$  and the thermal radiation parameter is referred to  $R$ , which can be defined as:

$$M = \frac{2L\sigma B_0}{\rho U_0}, \quad \lambda = \frac{2g\beta(T_w - T_\infty)L}{U_w^2}, \quad D = \frac{2\nu L}{U_w D^*}, \quad (10)$$

$$\text{Pr} = \frac{\mu c_p}{k}, \quad R = \frac{4\sigma^* T_\infty^3}{k^* k},$$

### 3. Keller-Box Method

Solving the analytical model of the nonlinear boundary layer equation for fluid mechanics is technically challenging. Keller-box approach is a viable option for solving a complex set of ODEs due to its excellent accuracy and speed in solving nonlinear equations. The Keller-box method is chosen to interpret Eq. (7) and Eq. (8) that were subject to the boundary equations of Eq. (9) as described by Cebeci and Bradshaw [25], Jamaludin *et al.*, [26, 27]. The recent studies by Jamshed *et al.*, [28, 29] acknowledged that the Keller-box have a swift convergence makes it effective for solving equations.

The Keller-box method contains three parts of the numerical method, which are finite difference method, Newton method and block elimination method.

Before all of that, the transformed ordinary differential equations in Eq. (7) and Eq. (8) are elucidate by transforming them to an initial value problem across the boundary conditions. The transformation process begins with introducing new variables of  $z = z(\eta)$ ,  $p = p(\eta)$ ,  $\theta = \theta(\eta)$  and  $q = q(\eta)$  as dependent variables. The new momentum and energy equations arrangement are as follow:

$$f' = z, \tag{11}$$

$$z' = p, \tag{12}$$

$$\theta' = q, \tag{13}$$

$$p' - 2z^2 + fp - Mz + \lambda\theta - Dz = 0, \tag{14}$$

$$\left(1 + \frac{4}{3}R\right)q' + \text{Pr}(fq - z\theta) = 0, \tag{15}$$

The boundary conditions in Eq. (9) in term of the new dependent variables then become:

$$f(0) = 0, \quad z(0) = 1, \quad \theta(0) = 1, \tag{16}$$

$$z(\infty) = 0, \quad \theta(\infty) = 0,$$

### 3.1 Finite Difference Method

The central differences are used to write the midpoint  $\eta_{j-1/2}$  of the segment  $\eta_{j-1}, \eta_j$  for the finite-difference approximations to the ordinary differential Eq. (11) to Eq. (15) [27]:

$$\frac{f_j - f_{j-1}}{h_j} = \frac{z_j + z_{j-1}}{2} = z_{j-1/2}, \tag{17}$$

$$\frac{z_j - z_{j-1}}{h_j} = \frac{p_j + p_{j-1}}{2} = p_{j-1/2}, \tag{18}$$

$$\frac{\theta_j - \theta_{j-1}}{h_j} = \frac{q_j + q_{j-1}}{2} = q_{j-1/2}, \tag{19}$$

$$\left(\frac{p_j - p_{j-1}}{h_j}\right) - 2(z_{j-1/2})^2 - Mz_{j-1/2} + f_{j-1/2}p_{j-1/2} + \lambda\theta_{j-1/2} - Dz_{j-1/2} = 0, \tag{20}$$

$$\left(1 + \frac{4}{3}R\right)\left(\frac{q_j - q_{j-1}}{h_j}\right) + \text{Pr}(f_{j-1/2}q_{j-1/2} - z_{j-1/2}\theta_{j-1/2}) = 0, \tag{21}$$

Rearranging the Eq. (17) to Eq. (21):

$$f_j - f_{j-1} - \frac{1}{2}h_j(z_j + z_{j-1}) = 0, \quad (22)$$

$$z_j - z_{j-1} - \frac{1}{2}h_j(p_j + p_{j-1}) = 0, \quad (23)$$

$$\theta_j - \theta_{j-1} - \frac{1}{2}h_j(q_j + q_{j-1}) = 0, \quad (24)$$

$$\left(\frac{p_j - p_{j-1}}{h_j}\right) - \frac{(z_j + z_{j-1})^2}{2} - \frac{M}{2}(z_j + z_{j-1}) + \frac{1}{4}(f_j + f_{j-1})(p_j + p_{j-1}) + \frac{\lambda}{2}(\theta_j + \theta_{j-1}) - \frac{D}{2}(z_j + z_{j-1}) = 0, \quad (25)$$

$$\left(1 + \frac{4}{3}R\right)\left(\frac{q_j - q_{j-1}}{h_j}\right) + \text{Pr}[(f_j + f_{j-1})(q_j + q_{j-1}) - (z_j + z_{j-1})(\theta_j + \theta_{j-1})] = 0, \quad (26)$$

While the boundary conditions in Eq. (16) turned to be as follows:

$$f_0 = 0, \quad z_0 = 1, \quad \theta_0 = 1, \quad (27)$$

$$z_j = 0, \quad \theta_j = 0,$$

### 3.2 Newton's Method

Aiming to solve the nonlinear system in Eq. (22) to Eq. (26), the Newton's method is used by introducing the following expressions from [25].

$$f_j^{(i+1)} = f_j^{(i)} + \delta f_j^{(i)}, z_j^{(i+1)} = z_j^{(i)} + \delta z_j^{(i)}, p_j^{(i+1)} = p_j^{(i)} + \delta p_j^{(i)}, \quad (28)$$

$$\theta_j^{(i+1)} = \theta_j^{(i)} + \delta \theta_j^{(i)}, q_j^{(i+1)} = q_j^{(i)} + \delta q_j^{(i)},$$

The superscript  $i$  and quadratic terms in  $\delta f_j^{(i)}$ ,  $\delta z_j^{(i)}$ ,  $\delta p_j^{(i)}$ ,  $\delta \theta_j^{(i)}$  and  $\delta q_j^{(i)}$  are dropped for simplicity following [25]. The equations of linear tridiagonal system obtained as follows:

$$\delta f_j - \delta f_{j-1} - \frac{1}{2}h_j(\delta z_j + \delta z_{j-1}) = (r_1)_{j-1/2}, \quad (29)$$

$$\delta z_j - \delta z_{j-1} - \frac{1}{2}h_j(\delta p_j + \delta p_{j-1}) = (r_2)_{j-1/2}, \quad (30)$$

$$\delta \theta_j - \delta \theta_{j-1} - \frac{1}{2}h_j(\delta q_j + \delta q_{j-1}) = (r_3)_{j-1/2}, \quad (31)$$

$$(a_1)_j \delta p_j - (a_2)_j \delta p_{j-1} - (a_3)_j \delta z_j - (a_4)_j \delta z_{j-1} + (a_5)_j \delta f_j + (a_6)_j \delta f_{j-1} + (a_7)_j \delta \theta_j + (a_8)_j \delta \theta_{j-1} = (r_4)_{j-1/2}, \quad (32)$$

$$\begin{aligned} & (b_1)_j \delta q_j - (b_2)_j \delta q_{j-1} + (b_3)_j \delta f_j + (b_4)_j \delta f_{j-1} - (b_5)_j \delta \theta_j \\ & - (b_6)_j \delta \theta_{j-1} - (b_7)_j \delta z_j - (b_8)_j \delta z_{j-1} = (r_5)_{j-\frac{1}{2}}, \end{aligned} \quad (33)$$

where

$$(a_1)_j = \frac{1}{h_j} + \frac{1}{2} f_{j-1/2}, (a_2)_j = \frac{1}{h_j} - \frac{1}{2} f_{j-1/2}, (a_3)_j = 2z_{j-\frac{1}{2}} + \frac{M}{2} + \frac{D}{2},$$

$$(a_4)_j = 2z_{j-1/2} + \frac{M}{2} + \frac{D}{2}, (a_5)_j = \frac{1}{2} p_{j-1/2}, (a_6)_j = \frac{1}{2} p_{j-1/2},$$

$$(a_7)_j = \frac{\lambda}{2}, (a_8)_j = \frac{\lambda}{2},$$

and

$$(b_1)_j = \left(1 + \frac{4}{3}R\right) \frac{1}{h_j} + \frac{1}{2} \text{Pr } f_{j-1/2}, (b_2)_j = \left(1 + \frac{4}{3}R\right) \frac{1}{h_j} - \frac{1}{2} \text{Pr } f_{j-1/2},$$

$$(b_3)_j = \frac{1}{2} \text{Pr } q_{j-1/2}, (b_4)_j = \frac{1}{2} \text{Pr } q_{j-1/2}, (b_5)_j = \frac{1}{2} \text{Pr } z_{j-1/2},$$

$$(b_6)_j = \frac{1}{2} \text{Pr } z_{j-1/2}, (b_7)_j = \frac{1}{2} \text{Pr } \theta_{j-1/2}, (b_8)_j = \frac{1}{2} \text{Pr } \theta_{j-1/2},$$

with

$$(r_1)_{j-1/2} = -(f_j - f_{j-1}) + h_j z_{j-\frac{1}{2}},$$

$$(r_2)_{j-1/2} = -(z_j - z_{j-1}) + h_j p_{j-\frac{1}{2}},$$

$$(r_3)_{j-1/2} = -(\theta_j - \theta_{j-1}) + h_j q_{j-\frac{1}{2}},$$

$$(r_4)_{j-1/2} = 2(z_{j-1/2})^2 - \frac{1}{h_j} (p_j - p_{j-1}) - (fp)_{j-\frac{1}{2}} + Mz_{j-\frac{1}{2}} - \lambda \theta_{j-\frac{1}{2}} + Dz_{j-\frac{1}{2}},$$

$$(r_5)_{j-1/2} = \left(1 + \frac{4}{3}R\right) \frac{1}{h_j} (q_j - q_{j-1}) - \text{Pr}(fq)_{j-\frac{1}{2}} + \text{Pr}(z\theta)_{j-\frac{1}{2}},$$

Boundary conditions can be represented as:

$$\delta f_0 = 0, \quad \delta z_0 = 0, \quad \delta \theta_0 = 0, \quad \delta z_j = 0, \quad \delta \theta_j = 0, \quad (34)$$

### 3.3 The Block Elimination Method

The block tridiagonal structure of the linearized difference Eq. (29) to Eq. (33) consists of either constants or variables. However, here it consists of block matrices. The elements of the matrices on constant wall temperature are defined as follows:

$$\begin{bmatrix} [A_1] & [C_1] & & & \\ [B_2] & [A_2] & [C_2] & & \\ & & \ddots & & \\ & & & \ddots & \\ & & & & [B_{J-1}] & [A_{J-1}] & [C_{J-1}] \\ & & & & & [B_{J-1}] & [A_{J-1}] \end{bmatrix} \begin{bmatrix} [\delta_1] \\ [\delta_2] \\ \vdots \\ [\delta_{J-1}] \\ [\delta_J] \end{bmatrix} = \begin{bmatrix} [r_1] \\ [r_2] \\ \vdots \\ [r_{J-1}] \\ [r_J] \end{bmatrix},$$

That is

$$[A][\delta] = [r], \tag{35}$$

where the elements of the matrices are as follows:

$$[A_1] = \begin{bmatrix} 0 & 0 & 1 & 0 & 0 \\ -\frac{1}{2}h_1 & 0 & 0 & -\frac{1}{2}h_1 & 0 \\ 0 & -\frac{1}{2}h_1 & 0 & 0 & -\frac{1}{2}h_1 \\ -(a_2)_1 & 0 & (a_5)_1 & (a_1)_1 & 0 \\ 0 & -(b_2)_1 & (b_3)_1 & 0 & (b_1)_1 \end{bmatrix},$$

$$[A_j] = \begin{bmatrix} -\frac{1}{2}h_{j-1} & 0 & 1 & 0 & 0 \\ -1 & 0 & 0 & -\frac{1}{2}h_{j-1} & 0 \\ 0 & -1 & 0 & 0 & -\frac{1}{2}h_{j-1} \\ (a_4)_{j-1} & (a_8)_{j-1} & (a_5)_{j-1} & (a_1)_{j-1} & 0 \\ 0 & 0 & (b_3)_{j-1} & 0 & (b_1)_{j-1} \end{bmatrix}, \quad 2 \leq j \leq J, \tag{36}$$

$$[B_j] = \begin{bmatrix} 0 & 0 & -1 & 0 & 0 \\ 0 & 0 & 0 & -\frac{1}{2}h_{j-1} & 0 \\ 0 & 0 & 0 & 0 & -\frac{1}{2}h_{j-1} \\ 0 & 0 & (a_6)_{j-1} & -(a_2)_{j-1} & 0 \\ 0 & 0 & (b_4)_{j-1} & 0 & -(b_2)_{j-1} \end{bmatrix}, \quad 2 \leq j \leq J, \tag{37}$$

$$[C_j] = \begin{bmatrix} -\frac{1}{2}h & 0 & 0 & 0 & 0 \\ 1 & 0 & 0 & 0 & 0 \\ 0 & 1 & 0 & 0 & 0 \\ -(a_3)_{j-1} & (a_7)_{j-1} & 0 & 0 & 0 \\ 0 & 0 & 0 & 0 & 0 \end{bmatrix}, \quad 1 \leq j \leq J-1, \tag{38}$$



$$[L][W] = [r], \quad (48)$$

where

$$[W] = \begin{bmatrix} [W_1] \\ [W_2] \\ \vdots \\ [W_{j-1}] \\ [W_j] \end{bmatrix}, \quad (49)$$

and the  $[W_j]$  are the  $5 \times 1$  column matrices. Next, the Eq. (48) was used to solve elements  $W$  as follows:

$$[\alpha_1][W_1] = [r_1], \quad (50)$$

$$[\alpha_j][W_j] = [r_j] - [B_j][W_{j-1}], \quad 2 \leq j \leq J, \quad (51)$$

The forward sweep is referred to the step in which  $\Gamma_j, \alpha_j$  and  $W_j$  are calculated. Then, the backwards sweep is used to gives the solution of  $\delta$  by the Eq. (47). The obtained elements of the following relations are:

$$[\delta_j] = [W_j], \quad (52)$$

$$[\delta_j] = [W_j] - [\Gamma_j][\delta_{j+1}], \quad 1 \leq j \leq J - 1, \quad (53)$$

The Eqs. (29) – (33) can be used to find the  $(i + 1)^{\text{th}}$  iteration in Eq. (28) by using the calculated elements of  $\delta$ . This routine calculates the fluid properties and, accounts for the boundary layer growth. Cebeci and Bradshaw [25] stated by using the wall shear parameter  $v_0$  as the convergence criterion, the convergence of the iterations can also be checked. For laminar flows, calculations are repeated until a convergence condition is met, and calculations cease when convergence is achieved as below.

$$|\delta v_0^{(i)}| < 10^{-5},$$

which gives about four-figure accuracy for most predicted quantities. The calculations are stopped when  $v_0$  becomes negative during any iteration.

#### 4. Results and Discussion

The numerical results are obtained based on the test run of Keller-box method through MATLAB by applying the boundary condition from Ishak [16] into the transformed equations. The results are discussed in parts depending on the governing parameters involved. Table 1 show the comparison of the heat transfer change by Bidin and Nazar [15] and Ishak [16] and the present result by manipulating the parameters of thermal radiation, magnetic and buoyancy. Noted that the local Nusselt number is the heat transfer rate and the permeability parameter,  $D$  is set into 0 since porous media will not be discussed in this study. The comparison between the previously published paper

and the present results are made in order to test the accuracy and the validity of the numerical results obtained. As been tabulated in Table 1, the numerical value of local Nusselt number  $-\theta'(0)$  in this research with different involvement of parameter  $R$ ,  $M$ ,  $\lambda$  and  $Pr$  in each case are in better agreement with the result published by Bidin and Nazar [15] and Ishak [16].

**Table 1**  
 Values of  $-\theta'(0)$  for different values of  $R$ ,  $M$ ,  $\lambda$  and  $Pr$

$R$	$M$	$\lambda$	$D$	$Pr$	Bidin and Nazar [15]	Ishak [16]	Present results
0.0	0.0	0.0	0.0	1.0	-0.9548	-0.9548	-0.9548
				2.0	-1.4714	-1.4715	-1.4715
				3.0	-1.8691	-1.8691	-1.8691
				5.0		-2.5001	-2.5002
0.0	1.0	0.0		1.0		-0.8611	-0.8596
		1.0					-0.9682
1.0	0.0	0.0			-0.5315	-0.5312	-0.5330
		1.0					-0.6520
1.0	1.0	0.0				-0.4505	-0.4570
		1.0					-0.5913

Figures 2 and 3 exhibit the velocity and thermal boundary layer for several buoyancy parameter values as parameter  $Pr$ ,  $R$  and  $M$  are equal to 1. Based on Figure 2, the velocity boundary layer thickness grows as  $\lambda$  increases, while the velocity boundary layer gradient at the surface, which represents the surface shear stress, decreases. As  $\lambda$  increases in Figure 3, the thermal boundary layer thickness decreases and the thermal boundary layer gradient develops. As a result of a drop in shear stress and an increase in temperature gradient, Table 2 reveals that the coefficient of surface friction reduces while the heat transfer rate increases.

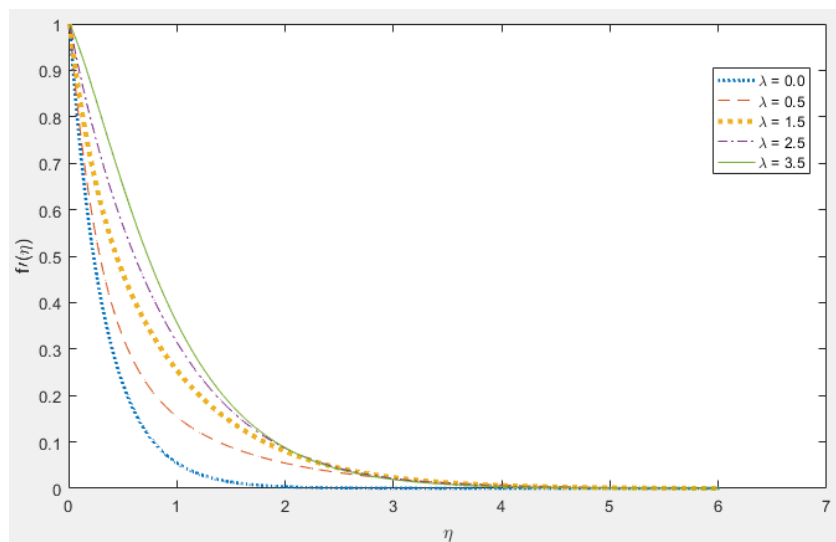


**Fig. 2.** Development of  $f'(\eta)$  for several point of  $\lambda$

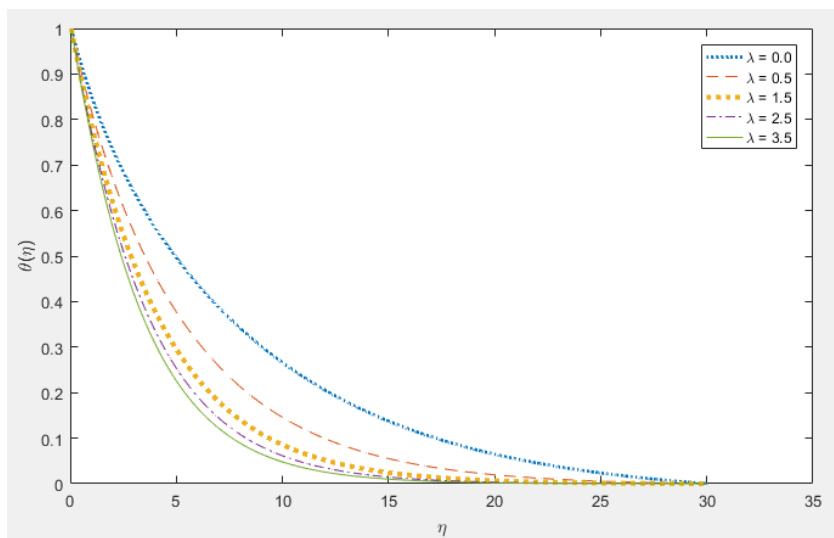


**Fig. 3.** Variant of  $\theta(\eta)$  for several point of  $\lambda$

**Table 2**

Characteristics of skin friction coefficient and heat transfer rate for varies of  $\lambda$  as  $Pr, M$  and  $R = 1$

$\lambda$	Skin friction coefficient	Heat transfer rate
0.0	1.6292	0.4570
0.5	1.3905	0.5461
1.5	0.9801	0.6241
2.5	0.6082	0.6728
3.5	0.2591	0.7099

Meanwhile, Figure 4 depicts the velocity boundary layer for several values of the magnetic parameter,  $M$  as  $\lambda, Pr$  and  $R$  are equal to 1. The thickness of the velocity boundary layer diminishes. The velocity boundary layer gradient rises, which causes the skin friction coefficient in Table 3 to rise. The decrease in transport rate is a result of the magnetic parameter increasing. It demonstrates that the transverse magnetic field resists transport phenomena due to the fact that Lorentz force produces resistance to transport phenomena in response to the variation of magnetic parameter.

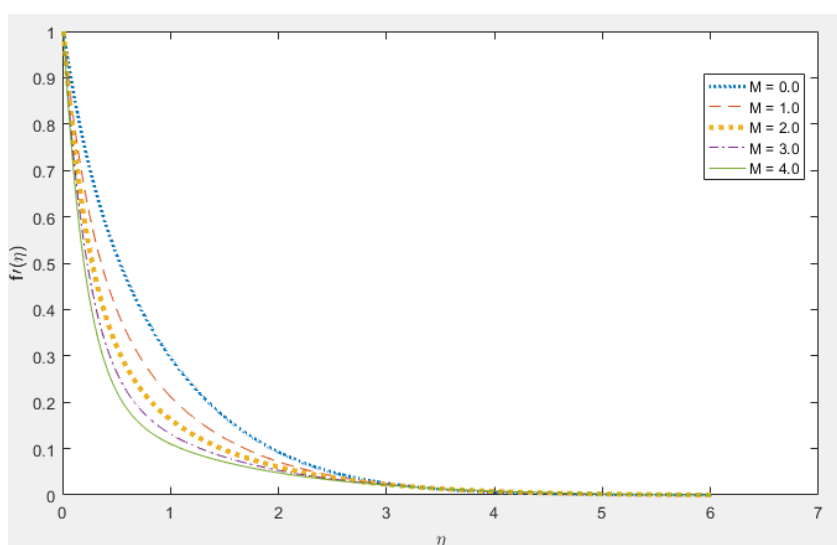


**Fig. 4.** Disparity of  $f'(\eta)$  for several point of  $M$

**Table 3**  
 Characteristics of skin friction coefficient and heat transfer rate for multiple values of  $M$  as  $\lambda, Pr$  and  $R = 1$

$M$	Skin friction coefficient	Heat transfer rate
0.0	0.7967	0.6520
1.0	1.1786	0.5913
2.0	1.4969	0.5436
3.0	1.7727	0.5053
4.0	2.0180	0.4740

Next, the thermal boundary layer can be seen in Figure 5 with multiple values of radiation parameter,  $R$ , as parameter  $\lambda, M$  and  $Pr$  are equal to 1. The thermal boundary layer found to be increases as  $R$  increases and led to the decrement in thermal boundary layer gradient. Table 4 shows the result commensurable to Figure 5 as it concludes the increasing of  $R$  cause the skin friction coefficient and heat transfer rate decreases in number.

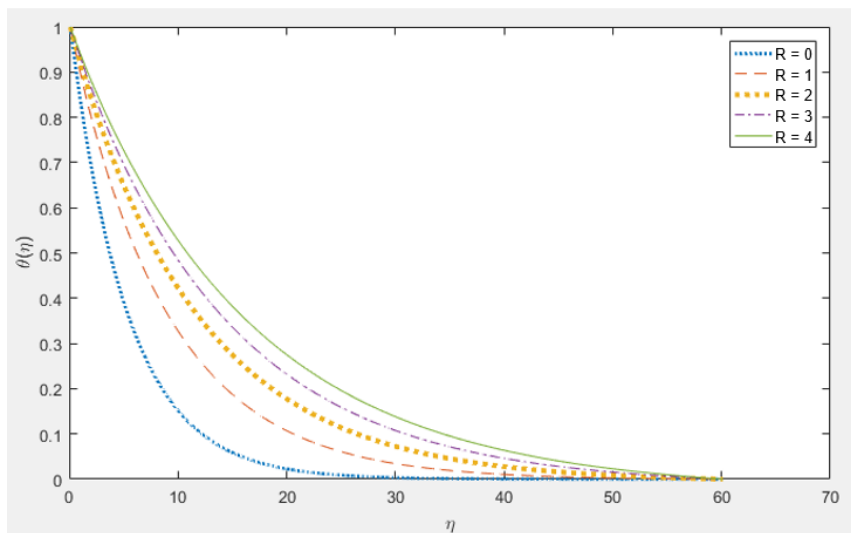


**Fig. 5.** Variation of  $\theta(\eta)$  for several point of  $R$

**Table 4**  
 Characteristics of skin friction coefficient and heat transfer rate for variation of  $R$  as  $\lambda, M$  and  $Pr = 1$

$R$	Skin friction coefficient	Heat transfer rate
0.0	1.2505	0.9682
1.0	1.1786	0.5913
2.0	1.1477	0.4567
3.0	1.1296	0.3837
4.0	1.1175	0.3367

Lastly, Figure 6 depicts the thermal boundary layer for various values of the Prandtl number,  $Pr$ , when the parameters of  $\lambda, R$  and  $M$  are equal to 1. As  $Pr$  grows, the thermal boundary layer thickness decreases, causing the thermal boundary layer gradient to increase. Table 5 demonstrates that an increase in  $Pr$  induces an increase in fluid viscosity and a decrease in thermal conductivity, which raises the skin friction coefficient and heat transfer rate.

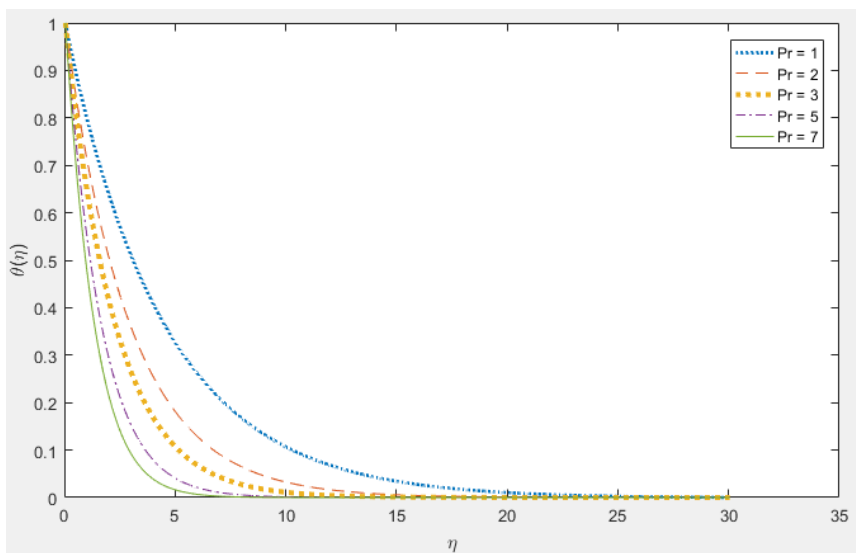


**Fig. 6.** Variant of  $\theta(\eta)$  for several point of Pr

**Table 5**

Characteristics of skin friction coefficient and heat transfer rate for different values of Pr as  $\lambda, M$  and  $R = 1$

$\lambda$	Skin friction coefficient	Heat transfer rate
1.0	1.1786	0.5913
2.0	1.2362	0.8847
3.0	1.2747	1.1217
5.0	1.3256	1.5113
7.0	1.3588	1.8354

## 5. Conclusions

In the present study, the laminar boundary layer flow and heat transfer across an exponentially extending sheet in the existence of buoyancy, magnetic field, and thermal radiation have been evaluated by applying established Keller-Box method. The accuracy of the results in this study has achieved agreement with the result published by Bidin and Nazar [15] and Ishak [16]. The increment of buoyancy parameter, speed up the fluid movement and promote the heat transfer rate. The presence of buoyancy in flow causes the surface shear stress decreases as  $M, R$  and Pr increases. However, the heat transfer rate of fluid found to be escalated as Pr increases.

## Acknowledgement

The authors immensely grateful to Universiti Teknologi MARA (UiTM) and Universiti Pertahanan Nasional Malaysia (UPNM) for supporting this research work. This research was funded by Universiti Pertahanan Nasional Malaysia via project codes of FRGS/1/2020/STG06/UPNM/03/1 and CRG/UPNM/2019/ST/04.

## References.

- [1] Idowu, A.S., and Usman, S. "Influence of Thermal Radiation on Magnetohydrodynamic (MHD) Boundary Layer Flow of a Viscous Fluid over an Exponentially Stretching Sheet." *International Journal of Applied Mechanics and Engineering* 21, no. 3 (2016): 581-592. <https://doi.org/10.1515/ijame-2016-0035>
- [2] Mushtaq, A., Farooq, M.A., Sharif, R., and Razzaq, M. "The Impact of Variable Fluid Properties on Hydromagnetic Boundary Layer and Heat Transfer Flows over an Exponentially Stretching Sheet." *Journal of Physics Communications* 3, no. 9 (2019): 095005. <https://doi.org/10.1088/2399-6528/ab31e2>

- [3] Loganathan, P., and Vimala, C. "MHD Boundary Layer Flow of a Nanofluid over an Exponentially Stretching Sheet in the Presence of Radiation." *Heat Transfer-Asian Research* 43, no. 4 (2014): 321-331. <https://doi.org/10.1002/htj.21077>
- [4] Asghar, Adnan, Teh Yuan Ying, and Khairy Zaimi. "Two-Dimensional Magnetized Mixed Convection Hybrid Nanofluid Over a Vertical Exponentially Shrinking Sheet by Thermal Radiation, Joule Heating, Velocity and Thermal Slip Conditions." *Journal of Advanced Research in Fluid Mechanics and Thermal Sciences* 95, no. 2 (2022): 159-179. <https://doi.org/10.37934/arfmts.95.2.159179>
- [5] Yusof, Nur Syamila, Siti Khuzaimah Soid, Mohd Rijal Ilias, Ahmad Sukri Abd Aziz, and Nor Ain Azeany Mohd Nasir. "Radiative Boundary Layer Flow of Casson Fluid Over an Exponentially Permeable Slippery Riga Plate with Viscous Dissipation." *Journal of Advanced Research in Applied Sciences and Engineering Technology* 21, no. 1 (2020): 41-51. <https://doi.org/10.37934/araset.21.1.4151>
- [6] Bakar, Fairul Naim Abu, and Siti Khuzaimah Soid. "MHD Stagnation-Point Flow and Heat Transfer Over an Exponentially Stretching/Shrinking Vertical Sheet in a Micropolar Fluid with a Buoyancy Effect." *Journal of Advanced Research in Numerical Heat Transfer* 8, no. 1 (2022): 50-55.
- [7] Rajput, G.R., Jadhav, B.P., and Salunkhe, S. "Magnetohydrodynamics Boundary Layer Flow and Heat Transfer in Porous Medium Past an Exponentially Stretching Sheet under the Influence of Radiation." *Heat Transfer* 49, no. 5 (2020): 2906-2920. <https://doi.org/10.1002/htj.21752>
- [8] Mahat, Rahimah, Muhammad Saqib, Imran Ulah, Sharidan Shafie, and Sharena Mohamad Isa. "MHD Mixed Convection of Viscoelastic Nanofluid Flow due to Constant Heat Flux." *Journal of Advanced Research in Numerical Heat Transfer* 9, no. 1 (2022): 19-25.
- [9] Ganesan, P., and Palani, G. "Finite Difference Analysis of Unsteady Natural Convection MHD Flow Past an Inclined Plate with Variable Surface Heat and Mass Flux." *International Journal of Heat and Mass Transfer* 47, no. 19-20 (2004): 4449-4457. <https://doi.org/10.1016/j.ijheatmasstransfer.2004.04.034>
- [10] Khan, Ansab Azam, Khairy Zaimi, Suliadi Firdaus Sufahani, and Mohammad Ferdows. "MHD flow and heat transfer of double stratified micropolar fluid over a vertical permeable shrinking/stretching sheet with chemical reaction and heat source." *Journal of Advanced Research in Applied Sciences and Engineering Technology* 21, no. 1 (2020): 1-14. <https://doi.org/10.37934/araset.21.1.114>
- [11] Hanafi, Hajar, and Sharidan Shafie. "Unsteady Free Convection MHD Flow over a Vertical Cone in Porous Media with Variable Heat and Mass Flux in Presence of Chemical Reaction." *Journal of Advanced Research in Fluid Mechanics and Thermal Sciences* 92, no. 2 (2022): 1-12. <https://doi.org/10.37934/arfmts.92.2.112>
- [12] Nayan, Asmahani, Nur Izzatie Farhana Ahmad Fauzan, Mohd Rijal Ilias, Shahida Farhan Zakaria, and Noor Hafizah Zainal Aznam. "Aligned Magnetohydrodynamics (MHD) Flow of Hybrid Nanofluid Over a Vertical Plate Through Porous Medium." *Journal of Advanced Research in Fluid Mechanics and Thermal Sciences* 92, no. 1 (2022): 51-64. <https://doi.org/10.37934/arfmts.92.1.5164>
- [13] Shafique, Ahmad, Muhammad Ramzan, Zaib Un Nisa, Mudassar Nazar, and Hafeez Ahmad. "Unsteady magnetohydrodynamic flow of second grade Nanofluid (Ag-Cu) with CPC fractional derivative: Nanofluid." *Journal of Advanced Research in Fluid Mechanics and Thermal Sciences* 97, no. 2 (2022): 103-114. <https://doi.org/10.37934/arfmts.97.2.103114>
- [14] Sajid, M., and Hayat, T. "Influence of Thermal Radiation on the Boundary Layer Flow due to an Exponentially Stretching Sheet." *International Communications in Heat and Mass Transfer* 35, no. 3 (2008): 347-356. <https://doi.org/10.1016/j.icheatmasstransfer.2007.08.006>
- [15] Bidin, Biliana, and Roslinda Nazar. "Numerical solution of the boundary layer flow over an exponentially stretching sheet with thermal radiation." *European journal of scientific research* 33, no. 4 (2009): 710-717.
- [16] Ishak, Anuar. "MHD boundary layer flow due to an exponentially stretching sheet with radiation effect." *Sains Malaysiana* 40, no. 4 (2011): 391-395.
- [17] Mukhopadhyay, S. "MHD Boundary Layer Flow and Heat Transfer over an Exponentially Stretching Sheet Embedded in a Thermally Stratified Medium." *Alexandria Engineering Journal* 52, no. 3 (2013): 259-265. <https://doi.org/10.1016/j.aej.2013.02.003>
- [18] Mukhopadhyay, S. "Slip Effects on MHD Boundary Layer Flow over an Exponentially Stretching Sheet with Suction/Blowing and Thermal Radiation." *Ain Shams Engineering Journal* 4, no. 3 (2013): 485-491. <https://doi.org/10.1016/j.asej.2012.10.007>
- [19] Lok, Y.Y., Amin, N., and Pop, I. "Mixed Convection near a Non-Orthogonal Stagnation Point Flow on a Vertical Plate with Uniform Surface Heat Flux." *Acta mechanica* 186, no. 1 (2006): 99-112. <https://doi.org/10.1007/s00707-006-0322-y>
- [20] Ishak, A., Nazar, R., and Pop, I. "MHD Mixed Convection Boundary Layer Flow Towards a Stretching Vertical Surface with Constant Wall Temperature." *International Journal of Heat and Mass Transfer* 53, no. 23-24 (2010): 5330-5334. <https://doi.org/10.1016/j.ijheatmasstransfer.2010.06.053>

- [21] Bhattacharyya, K., Mukhopadhyay, S., and Layek, G.C. "Similarity Solution of Mixed Convective Boundary Layer Slip Flow over a Vertical Plate." *Ain Shams Engineering Journal* 4, no. 2 (2013): 299-305. <https://doi.org/10.1016/j.asej.2012.09.003>
- [22] Daniel, Y.S., and Simon, K.D. "Effects of Buoyancy and Thermal Radiation on MHD Flow over a Stretching Porous Sheet Using Homotopy Analysis Method." *Alexandria Engineering Journal* 54, no. 3 (2015): 705-712. <https://doi.org/10.1016/j.aej.2015.03.029>
- [23] Ali, I. R., Ammar I. Alsabery, Norhaliza Abu Bakar, and Rozaini Roslan. "Mixed Convection in a Lid-Driven Horizontal Rectangular Cavity Filled with Hybrid Nanofluid by Finite Volume Method." *Journal of Advanced Research in Fluid Mechanics and Thermal Sciences* 93, no. 1 (2022): 110-122. <https://doi.org/10.37934/arfmts.93.1.110122>
- [24] Jahan, Sultana, M. Ferdows, M. D. Shamshuddin, and Khairy Zaimi. "Effects of Solar Radiation and Viscous Dissipation on Mixed Convective Non-Isothermal Hybrid Nanofluid over Moving Thin Needle." *Journal of Advanced Research in Micro and Nano Engineering* 3, no. 1 (2021): 1-11.
- [25] Cebeci, Tuncer, and Peter Bradshaw. *Physical and computational aspects of convective heat transfer*. Springer Science & Business Media, 2012.
- [26] Jamaludin, M.A, Nazar, R., and Shafie, S. "Numerical Solution of Heat Transfer Past a Stretching Sheet with Viscous Dissipation and Internal Heat Generation with Prescribed Surface Temperature." *AIP Conference Proceedings*, 2017. <https://doi.org/10.1063/1.4980921>
- [27] Jamaludin, A., Nazar, R., and Shafie, S. "Boundary Layer Flow and Heat Transfer in a Viscous Fluid over a Stretching Sheet with Viscous Dissipation, Internal Heat Generation and Prescribed Heat Flux." *AIP Conference Proceedings*, 2017. <https://doi.org/10.1063/1.4995861>
- [28] Jamshed, W., Prakash, M., Devi S., Ibrahim, R.W., Shahzad F., et al. "A Brief Comparative Examination of Tangent Hyperbolic Hybrid Nanofluid through a Extending Surface: Numerical Keller-Box Scheme." *Scientific Reports* 11, no. 1 (2021): 1-32. <https://doi.org/10.1038/s41598-021-03392-8>
- [29] Jamshed, W., Baleanu, D., Mohd Nasir, N.A.A., Shahzad, F., Nisar, K.S., et al. "The Improved Thermal Efficiency of Prandtl-Eyring Hybrid Nanofluid via Classical Keller Box Technique." *Scientific Reports* 11, no. 1 (2021): 1-24. <https://doi.org/10.1038/s41598-021-02756-4>